Structure and superconductivity in alkali tungsten bronzes

L. M. Kahn and J. Ruvalds
Physics Department, University of Virginia, Charlottesville, Virginia 22901
(Received 13 November 1978)

The anomalous concentration dependence of the superconducting transition temperature of alkali tungsten bronzes M_xWO_3 is shown to be consistent with electron pairing induced by exchange of acoustic plasmons. Structural changes in these metals yield significant band-structure splitting which is shown to be essential to the formation of well-defined acoustic-plasmon branches in the dielectric function. Our results explain why cubic H_xMO_3 is not superconducting even for large metallic densities $x \to 1$, and furthermore, demonstrate that the hexagonal phase is favorable to superconducting pairing in agreement with experiments on Rb_xWO_3 and Cs_xWO_3. Possible neutron and Brillouin scattering experiments are proposed to directly measure the acoustic-plasmon dispersion and damping.

I. INTRODUCTION

The alkali tungsten bronzes (of the form M_xWO_3 with M an alkali) as representatives of a group of narrow-band metal oxides (of the form M_xZO_3 where Z=W, Re, Ti, Ta...) are the focus of increasing study due to their intriguing electronic, structural, and optical properties.[1-7] These nonstoichiometric compounds are found to exist in cubic, hexagonal, and two types of tetragonal structures. The basic unit is the WO_3 octahedron, illustrated in Fig. 1. The stable structure is determined by the alkali concentration x and the size of the alkali. Thus, the small atoms, such as H, fit into the interstitial sites in the cubic phase shown in Fig. 2(a), whereas larger atoms like Rb induce a displacement to the hexagonal phase of Fig. 2(c). The intermediate case of Na_xWO_3 includes the tetragonal I structure shown in Fig. 2(b) as well as other phases depending on concentration.

Superconductivity in the alkali tungsten bronzes is remarkably sensitive to the alkali concentration and is strongly correlated with the crystal structure. For example, the cubic structure[8-10] does not exhibit a superconducting phase transition for any of the alkalis; and the case of H_xWO_3 is particularly anomalous since it remains normal even at highly metallic concentrations of $x \to 1$. On the other hand the hexagonal structure favors superconductivity in all of the alkalis tested to date. The current data on the superconducting transition temperatures is given in Table I.

Concentration variations of alkali content have a profound influence on the superconducting transition temperature T_c as shown in Fig. 3. The case of Rb_xWO_3 is particularly anomalous since T_c *increases* at lower concentrations, in contrast to the expectations of the BCS theory,[11] which predicts a decreasing T_c in accordance with the well-known relation

$$T_c \simeq \Theta_D \exp\left(-\frac{1}{gN(0)}\right), \tag{1}$$

where the Debye energy is $\Theta_D \simeq 300\,^\circ\mathrm{K}$, g is an electron-phonon matrix element and $N(0)$ denotes the electronic density of states at the Fermi energy. Experimentally, it is found that $N(0)$ increases roughly linearly with x (Refs. 10,12) and, therefore, T_c should also increase with x. In Fig. 3, this theoretical T_c based on an effective-mass model, is compared with experimental results for Rb and Na.[8-10] The obvious discrepancy becomes even more pronounced if $N(0) \propto x$ as indicated experimentally.

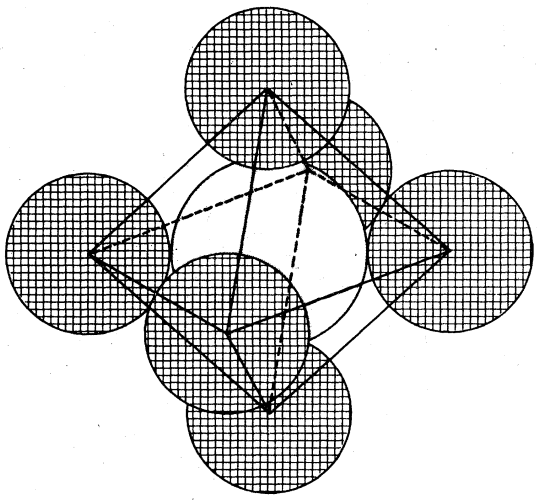

FIG. 1. Schematic representation of the octahedral structure of WO_3 is shown. The central atom (shaded) is tungsten. The remaining spheres (cross-hatched) represent the oxygen atoms.

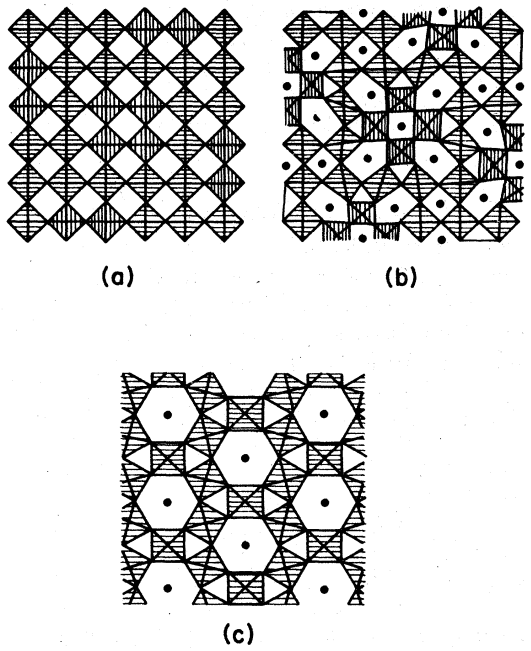

FIG. 2. Projections of the crystal structures of M_xWO_3 are illustrated for: (a) cubic, in this projection equivalent to tetragonal type 2, $T2$; (b) tetragonal type 1, $T1$; and (c) hexagonal. The dots represent the sites of the alkali M atoms. The octahedra, represented by shaded squares are those depicted in Fig. 1.

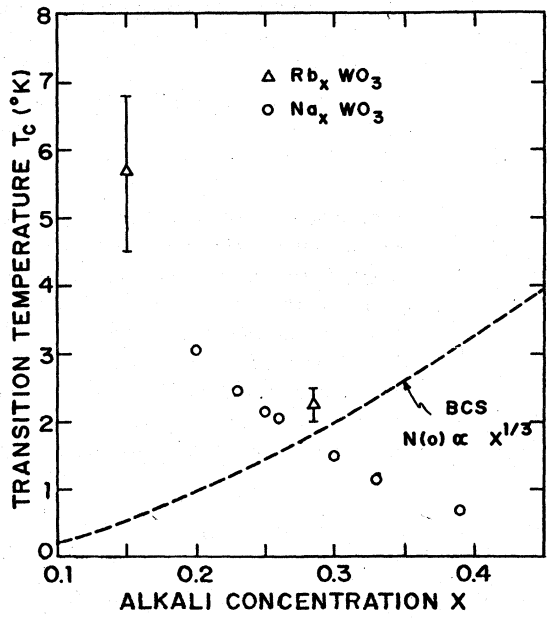

FIG. 3. Dependence of T_c on the concentration x for M_xWO_3 as determined experimentally is given for $M=$Na, Ref. 10, and $M=$Rb, Ref. 9. The theoretical curve is determined by the BCS expression $T_c \sim e^{-1/N(0)V}$ where $N(0) \propto x^{1/3}$.

An attempt was made to reconcile the anomalous concentration dependence with gross distortions of the phonon spectrum.[13] However, neutron data do not show soft modes that are strongly concentration dependent, thus indicating that other mechanisms should be considered.[14] It should be emphasized that any phonon mechanisms would require a variation of the coupling $g \propto x^{-2}$ in Eq. (1) to fit the T_c data, and such a dependence is hard to understand on physical grounds. Also, the similarity of the electronic band structure of all of the alkali tungsten bronzes, resembling ReO_3 in a rigid-band model, and of their $T_c(x)$ dependence seems to indicate the same mechanism is responsible for determining their superconducting transitions. A configuration change and accompanying phonon softening is not expected for Rb_xWO_3 in the region $0.15 < x < 0.33$ since Rb remains in the large hexagonal sites shown in Fig. 2.

TABLE I. Superconducting transition temperature in °K for M_xWO_3 structures.

M	Cubic	Tetragonal	Hexagonal
H	<0.35	<0.35($T2$)	?
Li	<0.35	<0.35($T2$)	1.3 – 2.2
Na	<0.35	0.8 – 3.1	1.3 – 5.4
K	· · ·	0.5 – 5.7	0.5 – 5.7
Rb	· · ·	· · ·	2.0 – 6.8
Cs	· · ·	· · ·	1.0 – 6.7

Lastly, the structural preferences of superconductivity in these materials is not at all evident from the phonon mechanism in the BCS theory.

The x dependence of T_c in the alkali tungsten bronzes initiated our interest in the possibility that the exchange of acoustic plasmons may be the mechanism for superconductivity. Preliminary work verified that the observed $T_c(x)$ could be theoretically reproduced using this mechanism.[15] In this paper we are primarily interested in relating the acoustic-plasmon mechanism to correlate the observed T_c with the structure of the compound, and to develop the criterion for the existence of acoustic branches in the electronic response.

Pines first suggested the existence of acoustic plasmons in a "two-plasma" system, which in our case is formed by the heavy and light electrons of the conduction band.[16] If the electrons were uncoupled, each would have a distinct finite plasmon frequency in the long-wavelength limit resulting from the long-range Coulomb interaction. However, if the plasmas are coupled, then under certain conditions, it is possible for the light-particle plasma to screen the heavy-

particle Coulomb interaction in such a way that, as in the case of phonons, an acoustic mode replaces the "optic" heavy-mass-plasmon mode.

In analogy with acoustic phonons, Fröhlich suggested that the exchange of acoustic plasmons as an electronic mechanism for superconductivity.[17] Within a simple effective-mass approximation, he derived conditions for the existence of acoustic plasmons and obtained a formula for the expected T_c. He found in general an increase in T_c with decreasing density, although he neglected the repulsive screened Coulomb potential. He also pointed out that the isotope effect would not be observed with this type of exchange and that T_c would roughly follow the Matthias rules for T_c versus electron per atom ratio,[18] since completely full or empty bands will not yield acoustic plasmons and the maximum frequency for an acoustic plasmon is greatest for half-filled shells.

Regrettably, little progress has been made in observing acoustic plasmons or determining superconductors which employ this mechanism. The difficulty in observation stems from their relatively low energy $\omega_p \lesssim 0.2$ eV. Electron scattering, while successfully able to detect higher-energy plasmons, is nearly out of range at this energy, due to background difficulties. Brillouin scattering of light may be used to detect well-defined acoustic plasmons, although no systematic evidence is available to date.

On the theoretical side, several papers have discussed the role plasmons might play in superconductivity of multiband semimetals[19,20] and transition metals.[21,22] The USSR literature refers mainly to high-temperature prospects of $T_c \sim 100\,^{\circ}$K, which requires unusually large mass ratios (say $m_d/m_s > 10$) and other restrictive parameters. Hence no attempt was made to correlate the calculations with known materials. By contrast, the previous work on transition metals presumed the existence of an acoustic plasmon with very *low* energy, even below the acoustic-phonon energies, and then examined the consequences of such low-lying modes on specific heat and other experimentally determined properties. The various observed anomalies may provide *indirect* evidence for the existence of acoustic plasmons in transition metals, but the correlation with the data is by no means certain.[21,22]

Recently we have proposed that the high-temperature superconductivity in A-15 compounds such as V_3Si may be a consequence of the acoustic-plasmon mechanism.[23] Here, the reduced dimensionality of the transition-metal chains is important. It was shown that the analytic structure of the dielectric function allowed acoustic plasmons to exist at all wavelengths for a system consisting of a linear chain, in a tight-binding model embedded in a free-electron gas of higher density. Choosing a model consistent with band-structure calculations, a superconducting phase transition mediated by acoustic plasmons was shown to occur at relatively high temperatures. While conceivable temperatures ranged as high as 100 K, the most realistic choice of parameters placed $T_c \sim 20$ K. This remarkable agreement has led us to search for other systems which may use the exchange of acoustic plasmons for superconductivity.

The purpose of the present work is to establish a correlation between structure and T_c, within the acoustic-plasmon model, for the tungsten bronzes. Specifically challenging is the case of H_xWO_3 which is found to have $T_c = 0$, while some other metal hydrides are very good superconductors with $T_c \simeq 17$ K. The plan of the paper is as follows. In Sec. II a simple two-band model is presented to establish the criteria governing the existence of acoustic plasmons. In Sec. III a realistic model for the alkali tungsten bronzes is investigated. The effects of reduced dimensionality are explored and the case of H_xWO_3 is investigated. Use of acoustic plasmons is shown to yield T_c in good agreement with experiment while allowing for an understanding of the structural dependence. Section IV comments on the limitation of high T_c are made alone with suggestions for possible experimental tests.

II. BASIC MODEL AND EQUATIONS

The existence of acoustic plasmons requires two overlapping electron bands corresponding to different effective masses. To make contact with the tungsten bronzes we display in Fig. 4 the band structure of

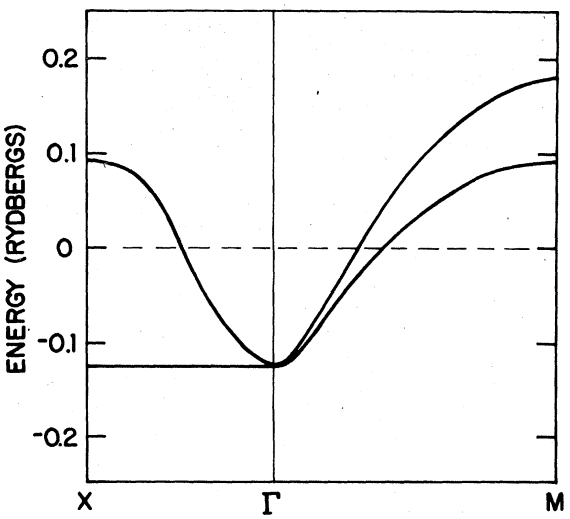

FIG. 4. Band structure of ReO_3 (from Ref. 24) is displayed as a prototype for M_xWO_3 with $x = 1$ and M, an alkali atom, in cubic structure. The success of the rigid-band model, where only the Fermi level (dashed line) changes with x has been demonstrated for cubic $NaWO_3$ which is nearly identical with ReO_3.

ReO_3 which corresponds to M_xWO_3 for $x=1$. Within the rigid-band model, decreasing x from $x=1$ corresponds to removing electrons from the conduction band of ReO_3.[24] Several band structure studies show this model to be well obeyed for many transition-metal oxides, in particular the alkali tungsten bronzes. In Fig. 4 the two dimensionality associated with the t_{2g} conduction bands is due to the planar nature of the $(pd\pi)$ interaction.[24] In the present section, we will constrain ourselves to a discussion of two overlapping electron bands in order to establish Fröhlich's criteria.

We describe the band structures by two effective masses with m_l denoting the lighter mass and m_h referring to the heavier mass. Generally the origins of these bands may be s or d like, but the present case of tungsten bronzes refers to both m_l and m_h originating from d bands.

The dielectric function for the model may be written

$$\epsilon_{\text{total}}(q,\omega)=\epsilon_0+Q_l(q,\omega)+Q_h(q,\omega)\ , \tag{2}$$

where Q_i is the Lindhard[25] polarizability for the i th band and ϵ_0 comprises all other contributions to the dielectric function. Following Fröhlich,[17] we note that the Q_i can be approximated by

$$Q_i(q,\omega)=\frac{k_{FT}^2}{q^2}\ ,\quad \text{for } q^2v_i^2>\omega^2\ , \tag{3a}$$

$$Q_i(q,\omega)=-\frac{\omega_{pi}^2}{\omega^2}\ ,\quad \text{for } q^2v_i^2<\omega^2\ , \tag{3b}$$

where $\omega_{pi}^2=4\pi n_i e^2/m_i^*$ is the plasmon frequency and v_i is the velocity at the Fermi energy of an electron in the i th band $(i=l,h)$, with $k_{FT}=(6\pi ne^2/E_F)^{1/2}$, as the Fermi-Thomas screening length. Therefore, in a region $qv_l>\omega>qv_h$, the approximate expression for the acoustic-plasmon frequency ω_{pa} is given by $\epsilon_{\text{total}}=0$ yielding

$$\omega_{pa}^2=\frac{q^2\omega_{ph}^2}{q^2\epsilon_0+3\omega_{pl}^2/v_l^2}\ , \tag{4}$$

which, in the limit of small q, has the form of an acoustic mode. Rewriting Eq. (2) and utilizing ω_{pa}, gives the simple form

$$\epsilon_{\text{total}}(q,\omega)=\epsilon_s(q)\left[1-\frac{\omega_{pa}^2}{\omega^2}\right]\ , \tag{5}$$

with

$$\epsilon_s(q)=\epsilon_0(q)+\frac{k_{FT}^2}{q^2}\ , \tag{6}$$

which is the dielectric constant when h electrons are neglected. Fröhlich's criteria are then written (a) $v_l^2>v_h^2$; and (b) $\epsilon_s(q_m)>0$, where q_m is the cutoff value of q, for which $\omega_{pa}^2=q^2v_h^2$; thus the plasmon is strongly damped for $q>q_m$. While these conditions are necessary they are not sufficient and should only be viewed as a rough indication of the region of parameters in which formation of acoustic plasmons occurs. A comparison of the approximate forms of $\epsilon(q,\omega)$ with the full Lindhard expression for ϵ_{total} shows that the computed acoustic-plasmon zero may be shifted by a factor of 2 as a result of the approximations; this may cause the acoustic plasmon to be Landau damped by the d continuum as shown in Fig. 5. Consequently we shall use the full Lindhard dielectric function in the calculations below, which is given by

$$\epsilon_i(q,\omega)=\frac{4\pi e^2}{q^2}\sum_{k\sigma}\frac{f(\vec{k}+\vec{q})-f(\vec{k})}{\omega-\omega(\vec{k}+\vec{q})+\omega(\vec{k})+i\delta}\ , \tag{7}$$

where $f(\vec{k})$ is the Fermi function. This reduces to

$$\text{Re}\,(\epsilon_i)=u^2\left\{\frac{1}{2}+\frac{1}{4y}\left[1-\left[\frac{z+y^2}{2y}\right]^2\right]\ln\left|\frac{z-2y+y^2}{z+2y+y^2}\right|+\frac{1}{4y}\left[1-\left[\frac{z-y^2}{2y}\right]^2\right]\ln\left|\frac{z-2y-y^2}{z+2y-y^2}\right|\right\} \tag{8a}$$

and

$$\text{Im}\,(\epsilon_i)=\begin{cases}\dfrac{zu^2\pi}{4y}\ ,\quad \text{for } 0\le z\le 2y-y^2\\ \dfrac{\pi u^2}{4y}\left[1-\left[\dfrac{z-y^2}{2y}\right]^2\right],\quad \text{for } 2y-y^2\le z\le 2y+y^2\ ,\\ 0\ ,\quad \text{for } z\ge 2y+y^2\end{cases} \tag{8b}$$

in the effective-mass approximation. Where the subscript i refers to the band index, with $z=\omega/E_F$, $y=q/k_F$, and $u=k_{FT}/q$ dimensionless parameters. E_F is the Fermi energy, and k_F is the Fermi momentum.

III. STRUCTURE

In the case of the system represented by the energy bands of Fig. 4, the degeneracy at the Γ point indicates a cubic, or tetragonal $T2$, structure. In this

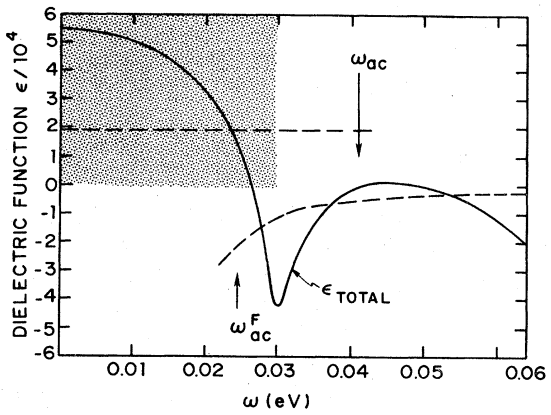

FIG. 5. Total dielectric function, $\epsilon_{\text{total}}(q, \omega)$, as calculated from the full Lindhard expression is displayed. The parameters determining the figure are $q = 0.28 \times 10^7$ cm^{-1}, $\xi = 0.14$ eV, $m_h = 3m_0$, $m_l = m_0$, and $x = 0.27$. The acoustic-plasmon frequency is given by ω_{ac}. The dashed lines represent the approximate dielectric function used by Fröhlich with the resulting acoustic plasmon labeled ω^F_{ac}. The shaded area represents the heavy-electron continuum.

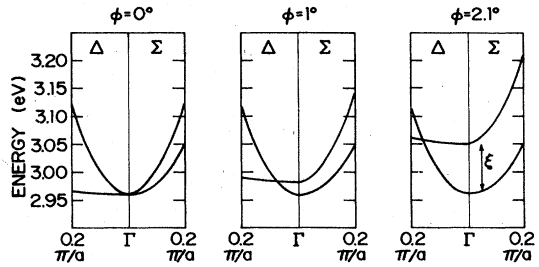

FIG. 6. Band structure of $SrTiO_3$ from Ref. 27 is shown for cubic structure ($\phi = 0°$; ϕ is the shift in position of the oxygen atoms) and two tetragonal structures; $\phi = 1°$, $\phi = 2.1°$. Note the 90 MeV splitting at Γ for $\phi = 2.1°$.

case, the heavy band will have a higher density than the light band for all x. While the Fröhlich criteria are satisfied, the calculations with the exact Lindhard function yield an acoustic-plasmon zero within the d continuum, thus yielding a highly damped excitation. Thus well-defined acoustic plasmons would not exist for the band model of Fig. 4 using $m_h/m_l = 3.0$. This model is precisely that encountered in H_xWO_3 at all but high pressures.[26] This is a result of the fact that hydrogen is sufficiently small that it does not require the large pentagonal or hexagonal sites accompanying the $T1$ or hexagonal structures which have a higher free energy that the $T2$ structure. Therefore, an acoustic-plasmon-induced electron attraction fails to exist for H_xWO_3 except perhaps under pressure, where hexagonal structures may occur. This is in agreement with experiment which shows no superconductivity for the alkali tungsten bronzes for cubic structures.

In light of the strict limitations imposed on the densities and the great similarity in band structure among transition-metal oxides, it might appear from the above result than the alkali tungsten bronzes are poor candidates for acoustic plasmons. In order to see the importance of structure in the determination of conditions governing the existence of acoustic plasmons, we refer to Fig. 6 which illustrates the analogous band structure of $SrTiO_3$ as calculated by Mattheiss.[27] He finds the effect of a cubic to tetragonal phase transition on the conduction bands is significant, even though transition involves only a 1–2° rotation of the oxygen atoms about Ti, from their cubic positions. As can be seen from Fig. 6 this slight rotation results in a 90 MeV shift of the Γ_5^+ state (heavy) with respect to the Γ_4^+ state (light). This shift, for reasonable effective masses and Fermi energies, is sufficient to guarantee the existence of acoustic plasmons in tungsten bronzes. Since the hexagonal and tetragonal Ti structures involve rotational angles larger than 2°, the splitting of levels is also expected to be larger than 90 MeV; and thus, the dependence of T_c on structure can be understood. We now put the above ideas in quantitative form.

To represent the noncubic crystal geometries a two-carrier band structure is used, given by

$$E_l = \frac{\hbar k^2}{2m_l}, \quad \text{and} \quad E_h = \xi + \frac{\hbar k^2}{2m_h}. \tag{9}$$

In the above expression ξ corresponds to the splitting between bands. Using this band structure to calculate the density of states at the Fermi level, $N(0) = N_l(0) + N_h(0)$ it is straightforward to show that, for a fixed electron density, $N(0)$ increases as ξ decreases. This implies that the cubic geometry, $\phi = 0°$, will have the largest $N(0)$. The BCS expression, $T_c \sim \Theta_D e^{-1/gN(0)}$, would, therefore, tend to favor the cubic geometry for higher transition temperatures if Θ_D remains relatively constant. This trend is contrary to the experimental results as described in Table I.

To achieve a quantitative understanding of the noncubic structures we incorporate the model of Eq. (9) together with the dielectric function of Eqs. (2) and (8). Choosing $m_l = m_0$ and $m_h = 3m_0$, where m_0 is the free electron mass, we obtain a domain in ξ and x for the existence of acoustic plasmons as shown in Fig. 7. It is interesting to note that the hexagonal structure with $\xi \simeq 0.1$ eV is bounded in x from above and below, thus allowing superconductivity from the present mechanism only over a limited concentration region.

The concentration dependence of the supercon-

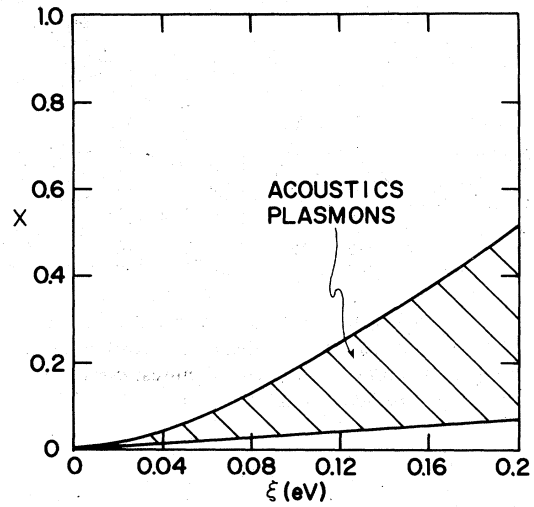

FIG. 7. Region where acoustic plasmons exist in $x-\xi$ space is indicated by the shaded area. ξ is the splitting between the two d bands as shown in Fig. 6, and x is the alkali concentration.

ducting transition temperature T_c is rather sensitive to the details of the plasma dispersion and the choice of the Coulomb potential screening.

The calculation of T_c for the acoustic-plasmon mechanism follows quite closely the standard calculation for phonons. As in the case of phonons, we are interested in the region where the electron-electron interaction becomes attractive due to the existence of an exchanged boson, the acoustic plasmon. The coupling between the electron and plasmon is simply the screened Coulomb interaction so that we can write the electron pairing contribution

$$V_{\text{el-el}} = \frac{4\pi e^2}{q^2 \epsilon_T(q,\omega)} . \tag{10}$$

Using Eq. (5) this can be rewritten

$$V_{\text{el-el}} \cong \frac{4\pi e^2}{q^2 \epsilon_s}\left(\frac{\omega_{ac}^2}{\omega^2-\omega_{ac}}+1\right) . \tag{11}$$

Here the first term is attractive for $\omega < \omega_{ac}$ while the second term is the screened Coulomb repulsion. This is similar in form to the attractive term which appears in phonon calculations with ω_{ac} replacing ω_{ph}. Application of the BCS formalism results in

$$T_c \simeq \Theta_{pl} \exp\left(\frac{-1}{F(x)-\mu^*}\right) , \tag{12}$$

where

$$F(x) = \frac{4\pi e^2}{q^2 \epsilon_s} N_T(0) \tag{13}$$

and the reduced Coulomb repulsion becomes[28]

$$\mu^* = \frac{\mu}{1+\mu \ln(E_F/\Theta_{pl})} , \tag{14}$$

with the Fermi-surface average of the Coulomb term represented by

$$\mu = \tfrac{1}{2}\int d(\cos\Theta)\frac{4\pi e^2}{q^2 \epsilon_s(q,0)} . \tag{15}$$

Θ_{pl} is the maximum acoustic-plasmon frequency in analogy with Θ_D for phonons.

As a consequence of the approximation of the attractive interaction by a square well in the BCS model, there is some uncertainty regarding the form of the density of states to be used in the expression

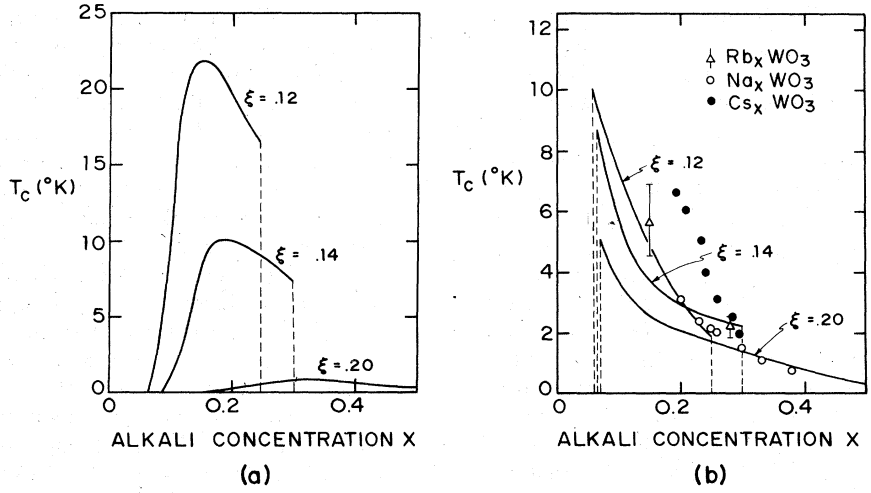

FIG. 8. Value of T_c as a function of concentration x is shown for two approximations of $F(x)$ discussed in the text: case (a) uses $F_a(x)$ from Eq. (16a), whereas (b) used $F_b(x)$ from Eq. (16b). In (b) we have superimposed the data from Fig. 3, as well as including more recent data on Cs_xWO_3 from Ref. 7.

for $N_T(0)$. Also the dielectric function can be evaluated at $q = q_m$ as suggested by Fröhlich, or at $q = k_f$ which alternately represents the screening. In Fig. 8 we display the results of two calculations of T_c with distinct representations for $F(x)$: In (a) we use the Fröhlich expression

$$F_a(x) = \frac{8\pi e^2}{q_m^2 \epsilon_s(q_m)} [N_l(0) N_h(0)]^{1/2} , \tag{16a}$$

and alternately in (b) we employ

$$F_b(x) = \frac{8\pi e^2}{q_m^2 \epsilon_s(k_F)} N_l(0) . \tag{16b}$$

The primary cause of the anomalous T_c dependence on concentration is the form of screening chosen for $F(x)$, since $\mu^* \simeq 0.17$ is essentially constant over the x range considered. However, $F(x)$ decreases slightly with x, in the case of

$$\xi = 0.12 \text{ eV}, \quad F_b(x = 0.08) = 0.34 ,$$

whereas $F_b(x = 0.23) = 0.31$, and naturally this dependence is amplified in T_c as seen in Eq. 12.

In view of the uncertainty of the various parameters involved a more sophisticated analysis of the Eliashberg equations seemed inappropriate. Nevertheless, quite good agreement is obtained for $T_c(x)$. The magnitude of the values of T_c as well as an increase in T_c as x decreases are representative of the experimental data.

It is interesting to note that the dependence of T_c on the energy splitting ξ is model dependent as shown in Fig. 8, so that detailed comparison with experiment requires more accurate band structures.

Finally, it is interesting to comment on the maximum value of T_c which can be expected from this model. We note that for a given set of parameters, T_c is limited either by the functional form of $F(x)$ or by the finite domain of existence of the acoustic plasmons. Because of the potentially large values of $\Theta_{pl} \gtrsim 3000$ K the opportunity for values of $T_c \sim 100$ K exists for modest values of the parameters. In general it is desirable to have $m_d/m_s >> 1$ while allowing densities which permit the existence of acoustic plasmons. As in the phonon case, strong coupling formulas will undoubtedly limit T_c to values considerably less than Θ_{pl}.

IV. DIRECT MEASUREMENTS OF ACOUSTIC PLASMONS

Central to the credibility of the acoustic-plasmon model of superconductivity is the observation of acoustic plasmons in those alkali tungsten bronzes which are superconductors and their absence in the nonsuperconductors. In this section we proceed to suggest experiments which hold promise of detecting the plasmons.

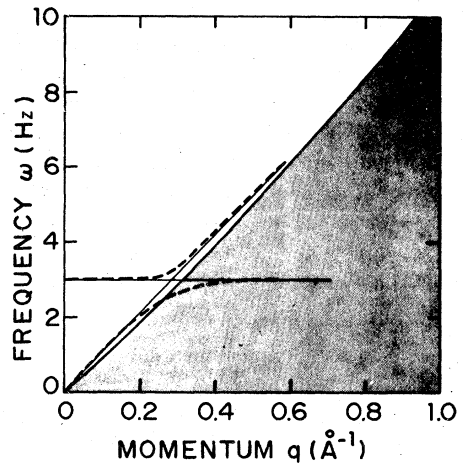

FIG. 9. Hybridization of an acoustic plasmon and an LO phonon is shown by dashed curves. The solid line represents the uncoupled dispersion of the phonon and plasmon. The shaded area represents the heavy-electron continuum and ω is in units of 10^{13} Hz.

Neutron scattering represents a means of observing plasmons at relatively large momenta. While neutrons do not couple strongly with the electrons, they do interact with phonons. In Fig. 9 we illustrate the dispersion of acoustic plasmons and phonons along

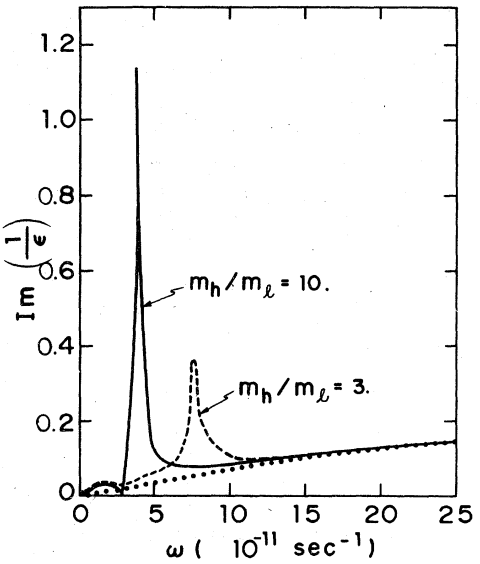

FIG. 10. Magnitude of Im $(1/\epsilon)$ is displayed for two electronic systems for small values of $q = 0.06 k_{Fl}$. The solid line is for $m_h/m_l = 10 (m_l = m_0)$ while the dashed line represents $m_h/m_l = 3$. The dotted line represents the magnitude Im $(1/\epsilon)$ in the absence of the h band. The band splitting is $\xi = 0.2$ eV and Im $(1/\epsilon)$ is in units of 10^{-5}. Here k_{Fl} is the Fermi momentum for the lighter mass electrons.

with longitudinal-optical (LO) phonons. The interaction betweeen the LO phonon and the acoustic plasmon will result in a hybridization of levels which should be observable either as a broadening of the LO level or a level splitting in the region of intersection, depending on the exact parameters involved. The structure factor should exhibit two peaks in ω by analogy with the polaron gas calculations.[29]

Brillouin scattering offers the possibility of observing the dispersion of the acoustic plasmon at small values of q. In this region the acoustic plasmon is a very well defined excitation as shown in Fig. 10. The dispersion for this range of q values should be $\omega \propto cq$, c being the constant velocity of the plasmon. At larger momenta the sampling of the acoustic-plasmon branch is significantly higher.

Finally, inelastic electron scattering, which has successfully been used to observe plasmons, may lend itself to the observation of acoustic plasmons. The relatively low energy of the acoustic plasmon may present some difficulty in its detection, but in principle the coupling should be strong, since its origin is the screened Coulomb interaction.

V. CONCLUSIONS

We have examined the superconductivity of the alkali tungsten bronzes and found substantial evidence that the electron pairing is induced by the exchange of acoustic plasmons. The conditions required for the existence of acoustic plasmons are determined by the structure of the crystal. Acoustic plasmons cannot occur in the cubic geometry; however, they are permitted in tetragonal and hexagonal geometries. Furthermore, it has been shown that higher transition temperatures result for hexagonal geometries than for tegragonal geometries when this mechanism is employed. These results are consistent with experiment as shown in Table I. In particular, the anomalous lack of a superconducting phase transition in H_xWO_3 can be understood, since it has cubic structure. Also, the calculated values for T_c are in good agreement with experiment for the various geometries.

Using this mechanism, it is possible to set an upper limit on the value of T_c for these materials. As was shown in Fig. 9, for a given value of the energy band splitting ξ, $T_c(x)$ has a maximum value of order 20 °K. This question naturally leads to the examination of maximum values of T_c obtainable through the acoustic-plasmon mechanism. Under ideal conditions it is possible to have acoustic plasmons with maximum frequencies $\omega_{pa} \sim 10^4$ °K. For these conditions, the calculation of T_c becomes somewhat more complicated. The difficulty which arises was well described by Inkson[30] in his study of superconductivity resulting from surface plasmons. He points out that low-energy boson excitations, which couple to the electrons, remove oscillator strength from the plasmon mode. The plasmon mode contributes to the screening of the repulsive Coulomb interaction, and thus, the treatment of an additional mode in the system must be carefully designed to avoid double counting. Therefore, extreme care is required in the calculation of μ^* to insure that the excitation used to pair electrons is not also counted upon to screen the repulsive interaction. Problems of this nature have resulted in controversy several times, most notably in the exciton mechanism for layered compounds postulated by Bardeen *et al.*[31] and discussed by Anderson and Inkson.[32]

For acoustic plasmons of reasonably small maximum frequency of the type in the present problem, the dominant screening comes from the "l" electrons and only a small contribution to the total oscillator strength comes from the acoustic plasmon, roughly 5%. Acoustic plasmons of higher frequency will be more significant in reducing the screening, however. This effect, which manifests itself in the exponent of the expression in Eq. (12), will tend to reduce the electron attraction and thus compensate for the increase in Θ_{pl}. The criterion for maximum T_c is uncertain. As mentioned earlier, there exists substantial literature, mainly in the Soviet Union,[19,20] which examine in an abstract sense the possibility of the acoustic-plasmon mechanism in multiband semiconductors. These calculations suggest $T_c = 100$ °K as a result of the large Θ_{pl} which may be attainable for very special band-structure parameters: The case of known alkali tungsten bronzes does not satisfy the extremely high T_c criterion.

The extension of the present analysis to transition metal superconductivity generally seems worthwhile. Our results discourage the expectations of a very low-lying plasmon mode of the type proposed by Rothwarf[21] and Ganguly.[22] They argued that an acoustic plasmon with energy *below* an acoustic-phonon energy would yield anomalous thermodynamic properties as well as possible distortions of the phonon spectrum. Our analysis shows that such low-lying modes require extremely low electron densities and very heavy effective masses: This conclusion is qualitatively apparent from the unscreened plasma frequency $\omega_h^2 = 4\pi n_h e^2/m_h^*$ of the heavy mass carriers. Since the acoustic phonons in some sense may be considered analogous to screened oscillations of the ion "plasma", the ratio n_h/m_h^* should be small compared to the corresponding ion density to mass ratio. Judging from available band-structure calculations of transition metals, these conditions are difficult to satisfy.

It is interesting to note that very low-energy acoustic plasmons with an effective Debye energy $\Theta_{pl} << 200$ °K would have a limited influence on the superconducting properties because of the limited

phase space for their existence. Nevertheless it may be interesting to apply the acoustic-plasmon mechanism to lightly doped semiconductors which are known to be superconducting at low temperatures.[33]

As a consequence of the relatively high plasmon "sound" velocities obtained in our calculations, these modes should have only a small influence on the thermodynamic properties of the tungsten bronzes.

Finally, we comment on possible extensions of the present theory. Generally speaking, our calculations indicate that the acoustic-plasmon damping in the tungsten bronzes is sufficiently small to have a negligible influence on T_c. Nevertheless the role of stronger damping will be considered in a future publication with particular emphasis on disorder and possible clustering effects[4] in the bronzes as well as other superconductors.

ACKNOWLEDGMENTS

It is a pleasure to acknowledge stimulating discussions with I. Tüttö, C. Friedberg, M. Cardona, J. T. Devreese, F. Brosens, L. Lemmens, I. Lefkowitz, and J. Snare. We are grateful to L. DeLong, A. Sweedler, and W. G. Moulton for very helpful data on the tungsten bronzes. This research was supported in part by the NSF Grant No. DMR77-13167.

[1]L. D. Ellerbeck, H. R. Shanks, P. H. Sidles, and G. C. Danielson, J. Chem. Phys. 35, 298 (1961).
[2]T. Wolfram, Phys. Rev. Lett. 29, 1383 (1972).
[3]I. Lefkowitz and G. W. Taylor, Opt. Commun. 15, 340 (1975).
[4]I. Wabman, J. Jortner, and M. H. Cohen, Phys. Rev. B 13, 713 (1976).
[5]C. N. King, J. A. Benda, R. L. Greene, and T. H. Geballe, *Low Temperature Physics - LT13*, edited by K. D. Timmerhaus, W. J. O'Sullivan and E. F. Hammel (Plenum, New York, 1972), Vol. III, p. 411.
[6]R. Silberglitt and L. H. Nosanow, Ferroelectrics 16, 275 (1977).
[7]R. K. Stanley, R. C. Morris, and W. G. Moulton (unpublished).
[8]A. R. Sweedler, C. J. Raub, and B. T. Matthias, Phys. Lett. 19, 82 (1965).
[9]A. R. Sweedler, Ph.D dissertation, (University of California, 1969) (unpublished).
[10]H. R. Shanks, Solid State Commun. 15, 753 (1974).
[11]J. Bardeen, L. N. Cooper, and J. R. Schrieffer, Phys. Rev. 106, 162 (1957); 108, 1175 (1957).
[12]F. Kupka and M. J. Sienko. J. Chem. Phys. 18, 1286 (1950).
[13]K. L. Ngai and R. Silberglitt, Phys. Rev. B 13, 1032 (1976).
[14]W. A. Kamitakahara, B. N. Harmon, J. G. Taylor, L. Kopp, H. R. Shanks, and J. Rath, Phys. Rev. Lett. 36, 1393 (1976).
[15]J. Ruvalds and L. M. Kahn, J. Phys. (Paris) 39, C6-460 (1978).
[16]D. Pines, Can. J. Phys. 34, 1379 (1956).
[17]H. Fröhlich, J. Phys. C 1, 544 (1968).
[18]B. T. Matthias, Phys. Today 24, 21 (1971).
[19]B. T. Geilikman, Sov. Phys. Solid State 12, 1497 (1971).
[20]E. A. Pashitskii, V. L. Makarov, and S. D. Tereshchenko, Sov. Phys. Solid State 16, 276 (1974); E. A. Pashitskii and V. M. Chernousenko, Zh. Eksp. Teor. Fiz. [Sov. Phys. JETP 33, 802 (1971)].
[21]A. Rothwarf, Phys. Rev. B 2, 3560 (1970).
[22]B. N. Ganguly and R. F. Wood, Phys. Rev. Lett. 28, 681 (1972).
[23]J. Ruvalds and L. M. Kahn (unpublished).
[24]L. F. Mattheiss, Phys. Rev. 181, 987 (1969); B 2, 3918 (1970). Also see: L. Kopp, B. N. Harmon, and S. H. Liu, Solid State Commun. 22, 677 (1977).
[25]J. Lindhard, K. Dan. Vidensk. Selsk. Mat. Fsy. Medd. 28, No. 8 (1954).
[26]T. E. Gier, D. C. Pease, A. W. Sleight, and T. A. Bither, Inorg. Chem. 7, 1646 (1968).
[27]L. F. Mattheiss, Phys. Rev. B 6, 4740 (1972).
[28]N. N. Bogoliubov, V. V. Tolmachev, and D. V. Shirkov, *A New Method in the Theory of Superconductivity* (Consultants Bureau, New York, 1958).
[29]L. F. Lemmens, F. Brosens, and J. T. Devreese, Solid State Commun. 17, 337 (1975).
[30]J. C. Inkson, J. Phys. C 8, L164 (1975).
[31]D. Allender, J. Bray, and J. Bardeen, Phys. Rev. B 7, 1020 (1973); B 8, 4433 (1973).
[32]J. C. Inkson and P. W. Anderson, Phys. Rev. B 8, 4429 (1973).
[33]R. A. Hein, J. W. Gibson, R. L. Falge, Jr., R. L. Mazelsky, R. C. Miller, and J. K. Hulm, Proceedings of International Conference on Semiconducting Physics, Kyoto, 1966 (unpublished).

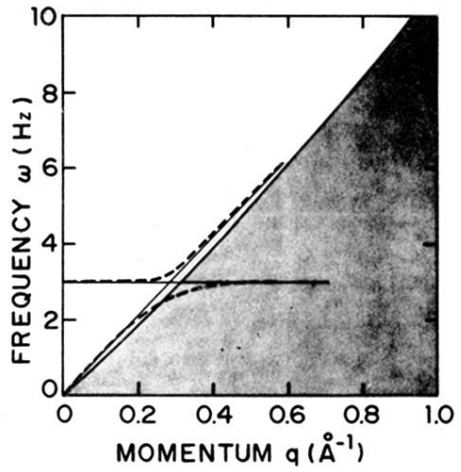

FIG. 9. Hybridization of an acoustic plasmon and an LO phonon is shown by dashed curves. The solid line represents the uncoupled dispersion of the phonon and plasmon. The shaded area represents the heavy-electron continuum and ω is in units of 10^{13} Hz.